Scientia Iranica A (2021) 28(2), 645–655

Sharif University of Technology
Scientia Iranica
Transactions A: Civil Engineering
http://scientiairanica.sharif.edu

Prediction of discharge flow rate beneath sheet piles using scaled boundary finite element modeling database

A. Johari*, A. Heydari, and A. Talebi

Department of Civil and Environmental Engineering, Shiraz University of Technology, Shiraz, P.O. Box 71557-13876, Iran.

Received 6 April 2019; received in revised form 23 June 2019; accepted 11 January 2020

KEYWORDS
Seepage;
Scaled boundary finite-element method;
Flow rate discharge;
Sheet pile;
Gene expression programming.

Abstract. Sheet piles are of general water-retaining structures. The rate of discharge flow beneath sheet plies is an important parameter in the design of these structures. In this study, Gene Expression Programming (GEP) as an artificial intelligence method is used for developing a model to predict the discharge flow rate. The input parameters include the sheet pile height, upstream head, and hydraulic conductivity anisotropy ratio. In order to achieve better performance, the flow rate is normalized and selected as an output of the model. A database including 1000 cases created from the Scaled Boundary Finite Element Method (SBFEM) for the seepage beneath sheet plies is employed to develop the model. The GEP-based model predictions are shown in reasonable agreement with the simulated data, which indicates the efficiency of the developed model. The results of the sensitivity analysis indicate that the upstream head is the most influential parameter in the discharge flow rate beneath the sheet piles. Furthermore, the outputs of the parametric analysis show the reasonable performance of the model in the prediction of normalized discharge flow rate.

1. Introduction

Desirable safety of water-retaining structures has always been among the most primary concerns in civil engineering. The discharge flow rate on the downstream side of a water-retaining structure as a seepage output quantity plays a fundamental role in the safe design of the structure. The stability of the water-retaining structures can be endangered by high values of the discharge flow. Sheet pile is has vital structures installed in a flow region or under the foundation of a dam to reduce the values of downstream discharge flow rate. The discharge flow rate is calculated using seepage analysis. Similar to most of the problems in geotechnical engineering, the seepage beneath sheet pile follows a specific differential equation. Various methods have been employed by researchers to solve the seepage governing equation and therefore, compute the flow rate discharge. Among the contributions, the analytical and numerical methods have been performed more broadly.

He [1] suggested a variational iteration method with fractional derivatives as an analytical method to solve the nonlinear seepage flow into porous media. Jie et al. [2] handled a finite difference method based on boundary-fitted coordinate transformation to analyze the steady-state seepage with a free surface of the isotropic and homogeneous embanked dam. Fukuchi [3] employed a so-called boundary polynomial interpo-

*. *Corresponding author.*
E-mail addresses: johari@sutech.ac.ir (A. Johari); heydari.ahmed@gmail.com (A. Heydari); a.talebi@sutech.ac.ir (A. Talebi)

doi: 10.24200/sci.2020.53281.3158

lation finite difference method to analyze the two- and three-dimensional seepage problems. Bresciani et al. [4] suggested two practical approaches that rely on finite volume method to find viable solutions to groundwater flow problems through earth dams. The methods enjoy the most beneficial advantages of adaptive and fixed mesh methods, combined. Ouria et al. [5] employed a coupled finite element method to model the transient seepage flow beneath a concrete dam. Kazemzadeh-Parsi and Daneshmand [6] exerted a smoothed fixed grid finite element method to analyze three-dimensional unconfined seepage of complex geometries in heterogeneous and anisotropic porous media. Rafiezadeh and Ataie-Ashtiani [7] developed a coded computer program based on the boundary element method to analyze three-dimensional confined seepage problems under dams. Jie et al. [8] simulated the unconfined seepage problems using natural element method. The node locations were arbitrary in this meshless method and, therefore, the seepage problems with a free surface could be properly analyzed. Zhang et al. [9] exercised a method based on mesh-free technique to analyze the free surface seepage problem as a moving boundary problem. The moving Kriging interpolation was used to create shape functions.

The analytical techniques have the potential to provide an exact solution, while these methods cannot straightly apply to the problems of complicated geometries and complex boundary conditions. However, numerical methods provide approximate analyses that enjoy high accuracy in dealing with more sophisticated problems. The finite difference, finite volume, and finite element approaches are considered as mesh-based methods required to discretize the whole problem domains. The importance of this disadvantage becomes more evident when one encounters a domain consisting of singular points and sharp corners.

More recently, a newfound semi-analytical method is called Scaled Boundary Finite Element Method (SBFEM), which has been contrived by Song and Wolf [10] to transcend the limits of the mentioned approaches. The SBFEM is properly capable to solve different types of differential equations. The SBFEM merges important merits of the finite element and the boundary element methods. Bazyar and Graili [11] analyzed the confined seepage problems beneath the dams and the sheet piles in steady-state conditions in anisotropic media using SBFEM. In another part of this study, unconfined flow problems with the unknown free surface through the dam body were investigated. Bazyar and Talebi [12] extended the SBFEM to analyze the transient seepage problems in bounded and unconfined domains. The proposed method was capable of solving the heterogeneous and anisotropic porous media with convenience. Johari and Heydari [13] carried out reliability analysis of seepage in several numerical problems through stochastic SBFEM. Su et al. [14] utilized drainage substructure and nodal virtual flux method to simulate drainage holes and analyze complex seepage fields.

Based on the advantages of the SBFEM, it seems to be a practical method for analyzing the seepage beneath sheet plies and determining the discharge flow rate. Despite the efficiency of the SBFEM in obtaining the discharge flow rate, a separate analysis is required to compute the discharge flow rate in every single condition. Furthermore, the user must be fully acquainted with the analysis procedure to analyze the seepage problem beneath the sheet piles and, subsequently, determine the discharge flow rate. For these reasons, prediction models have been developed to directly associate the quantities, e.g., discharge flow rate, to effective parameters, hence obviating unnecessary need for any analytical, numerical, or laboratory methods to calculate the discharge flow rate. Therefore, data-driven approaches, regression methods, artificial intelligence, and other soft computing techniques have recently drawn much attention to generating prediction equations. Artificial Neural Networks (ANN) [15,16], Adaptive Neuro-Fuzzy Inference System (ANFIS) [17,18], Ant Colony Optimization (ACO) [19], Evolutionary Polynomial Regression (EPR) [20], Genetic Algorithm (GA) [21–23], Genetic Programming (GP) [24–27], Genetic-Based Neural Network (GBNN) [28,29], and Gene Expression Programming (GEP) [30–32] can be mentioned as the most conventional soft computing and heretofore outstanding contributions in various civil engineering problems.

Despite several types of research on predicting the discharge flow rate beneath the sheet pile, limited powerful numerical models such as the SBFEM have been used for creating a database of GEP modeling. In this research, using the advantages of SBFEM, the database was created and verified by the results of the FEM analysis. The database of discharge flow rate includes 1000 data for different values of input parameters such as sheet pile's height, upstream water level, and hydraulic conductivity anisotropy ratio of the material. Performance analysis was applied to find the optimum parameters of the GEP model. Some different models based on various functions were obtained and then, by comparing the relative errors of different models, one of these models was selected as the proposed one. Furthermore, the most effective input parameter of the proposed model was determined.

2. Steady-state two-dimensional seepage

The seepage flow beneath water-retaining structures constructs nonlinear streamlines for which Darcy's law cannot be used directly. The steady-state seepage

flow through porous media can be represented as follows [33]:

$$\nabla \cdot [[k]\nabla h] = 0, \tag{1}$$

where ∇ represents the differential operator; $[k]$ and h are the tensor of hydraulic conductivity and hydraulic head, respectively.

Flow rate, exit gradient, and safety factor against piping are important quantities that can be obtained by analyzing the seepage flow problems.

3. The Scaled Boundary Finite-Element Method (SBFEM)

The method is semianalytical and only needs discretization of the boundary of the problem. Unlike the conventional Finite Element Method (FEM) which limits the type of discretization to simplex shapes, the SBFEM allows discretization with arbitrary sided polygons subjected to a scaling center. This geometric requirement can always be satisfied by dividing the domain into subdomains [34]. To describe the domain of the problem, the Cartesian coordinates are transformed into SBFEM radial and circumferential coordinates ξ, η. By using this method, the points located in adjacency to sharp corners or singular points can be modeled directly with high accuracy. This feature can be utilized to model seepage beneath the sheet piles by considering the center of subdomain generation beneath the water-retaining structures. According to the Galerkin's weighted residual method, the SBFEM equation in terms of head function can be obtained as follows [35]:

$$\left[E^0\right]\xi^2\frac{\partial^2\{h(\xi)\}}{\partial\xi^2}+\left(\left[E^0\right]-\left[E^1\right]+\left[E^1\right]^T\right)\xi\frac{\partial\{h(\xi)\}}{\partial\xi} - \left[E^2\right]\{h(\xi)\} = 0, \tag{2}$$

where $\{h(\xi)\}$ is the head function and $[E^0]$, $[E^1]$, and $[E^2]$ are coefficient matrices as follows:

$$\left[E^0\right] = \int_\eta \left[B^1(\eta)\right]^T [k] \left[B^1(\eta)\right] |J| d\eta, \tag{3}$$

$$\left[E^1\right] = \int_\eta \left[B^2(\eta)\right]^T [k] \left[B^1(\eta)\right] |J| d\eta, \tag{4}$$

$$\left[E^2\right] = \int_\eta \left[B^2(\eta)\right]^T [k] \left[B^2(\eta)\right] |J| d\eta, \tag{5}$$

where $[E^0]$, $[E^2]$, and $[E^1]$ are positive definite, semi-positive definite, and non-symmetric matrices, respectively. $[k]$ is the hydraulic conductivity tensor. $[B^1(\eta)]$ and $[B^2(\eta)]$ represent the head gradient-head relationship as follows:

$$\left[B^1(\eta)\right] = \frac{1}{|J|}\begin{Bmatrix}\frac{\partial y(\eta)}{\partial\eta}\\ \frac{-\partial x(\eta)}{\partial\eta}\end{Bmatrix}[N(\eta)], \tag{6}$$

$$\left[B^2(\eta)\right] = \frac{1}{|J|}\begin{Bmatrix}-y(\eta)\\ x(\eta)\end{Bmatrix}\frac{\partial[N(\eta)]}{\partial\eta}. \tag{7}$$

$|J|$ is the determinant of the Jacobian matrix on the boundary and can be expressed as follows:

$$|J| = x(\eta)\frac{\partial y(\eta)}{\partial\eta} - y(\eta)\frac{\partial x(\eta)}{\partial\eta}. \tag{8}$$

The Cauchy-Euler equation in Eq. (2) leads to a linear eigenvalue problem as [36]:

$$\begin{bmatrix}\left[E^0\right]^{-1}\left[E^1\right]^T & -\left[E^0\right]^{-1}\\ -\left[E^2\right]+\left[E^1\right]\left[E^0\right]^{-1}\left[E^1\right]^T & -\left[E^1\right]\left[E^0\right]^{-1}\end{bmatrix} \begin{bmatrix}[\phi_{11}] & [\phi_{12}]\\ [\phi_{21}] & [\phi_{22}]\end{bmatrix} = \begin{bmatrix}[\phi_{11}] & [\phi_{12}]\\ [\phi_{21}] & [\phi_{22}]\end{bmatrix}\begin{bmatrix}[\lambda] & \\ & -[\lambda]\end{bmatrix}. \tag{9}$$

The stiffness matrix is determined as follows:

$$[K] = [\phi_{21}][\phi_{11}]^{-1}. \tag{10}$$

The nodal heads on the boundary are determined using the nodal head-flow rate relation, which is formulated as follows:

$$\{Q\} = [K]\{h\}. \tag{11}$$

The nodal flow rates are obtained using Eq. (11) and determined nodal heads. The total flow rate can be computed by calculating the sum of downstream boundary nodal flow rates. In order to achieve better evaluation, the flow rate is calculated in the dimensionless form as follows:

$$Q_{Nor.} = \frac{Q}{\mu_k \Delta h}, \tag{12}$$

where $Q_{Nor.}$ is a non-dimensional flow rate, μ_k is the mean of conductivity, and Δ_h is the difference between the values of the head at upstream and downstream of the dam.

4. Gene Expression Programming (GEP)

GEP, a fully-fledged computer program to meet the best-fitted models, is an evolved artificial intelligence method and a recent GP development. GEP has integrated the features of both GP and GA techniques

along with introducing their unique advantages. Similar to GA, GEP engenders programs of the codified linear individuals (chromosomes) with a fixed length. The chromosomes are divaricated into nonlinear structures with varied sizes and shapes like the parse trees of GP [37].

The procedure commences with random generation of chromosomes from a preliminary population. Every single chromosome comprises variables (terminal) and different mathematical functions (e.g., +, −, etc.). The chromosome expresses and converts into computer programs. The generated programs are implemented, the performance of which is evaluated according to their desirable fitness function. Programs with the best performance are selected. The next step consists of a reproduction of new chromosomes through the best-performing individual programs using genetic operators including replication, mutation, inversion, gene transposition, and recombination. If the cessation conditions are met, the process can be terminated at this step; otherwise, the process has to be repeated until the termination criterion is met.

The chromosome comprises one or more genes. Each gene possesses two types of information. The first type represents the information used for creating the overall GEP model, which is stored in the head of the genes. The second type is the tail information and contains only terminals. Genes can be connected by linear functions. A presentation of a sample chromosome is depicted in Figure 1. The chromosomes are read from the left to the right direction and then, top to bottom.

5. Model developing methodology

Since no database for sheet piles has been presented in literature so far, the first step in this research is to provide a database for developing models using GEP. For this reason, the SBFEM as a robust semi-analytical method was employed. As mentioned before, one of the important advantages of this method is modeling the singular points directly with high accuracy. This feature can be utilized to model seepage beneath the sheet piles as a singular point. Figure 2 shows the geometry and the boundary condition of the problem domain, which is divided into non-uniform subdomains. The sheet pile is considered in the middle of the modeling. A 20.0 m by 40.0 m horizontal saturated soil is modeled as the domain of the problem. The domain is discretized into 450 triangle subdomains. Each side of the subdomains is discretized by two nodded linear elements. The scaling centers related to corresponding subdomains are located exactly at the geometry center. In terms of boundary conditions, the base as well as left and right sides of the soil layer are fully impermeable.

5.1. Verification of the SBFEM model

In this section, a general example of seepage flow beneath a sheet pile is presented to assess the efficiency of the SBFEM model. The preciseness and versatility of the model are clarified based on the comparison between the results of SBFEM with those of FEM. For this purpose, another coded program based on FEM is provided by the authors to verify the model's accuracy. The domain discretization for both models is shown in Figures 3 and 4. The domain is discretized into 450 subdomains and 3200 elements for SBFEM and FEM, respectively. The contour of potential lines for the results of SBFEM and FEM is demonstrated in Figure 5. The findings indicate great compatibility between the outcomes of SBFEM and FEM.

Moreover, for verification, 10 simple flow rates of the database related to different scenarios are expressed in Table 1. The results indicate great compatibility between the results of the dataset and those of FEM.

5.2. Database

In this section, a general sheet pile is considered to prepare a dataset of 1000 possible scenarios under various boundary conditions. The geometry of the sheet pile is portrayed in Figure 2. Three independent

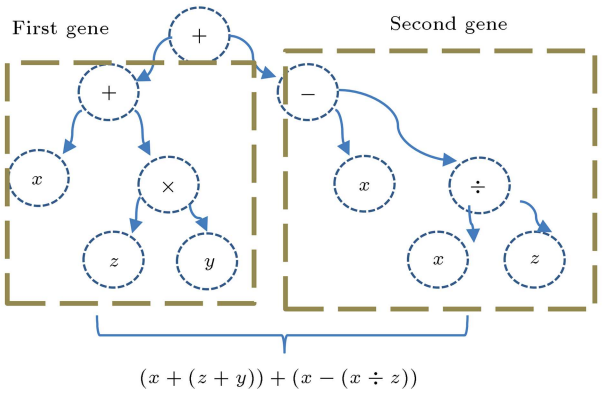

Figure 1. A sample chromosome.

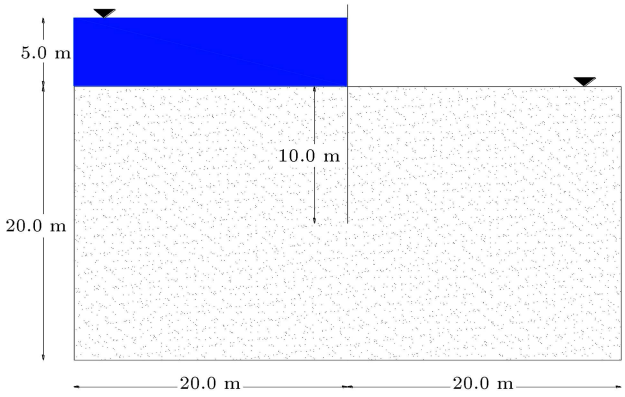

Figure 2. The geometry of the model.

Table 1. Ten simple values of the dataset.

Upstream head (H)	Sheet pile's height (D)	Hydraulic conductivity anisotropy ratio (K)	Normalized flow rate ($Q_{Nor.}$) (SBFEM)	Normalized flow rate ($Q_{Nor.}$) (FEM)
1	0.5	0.4	8.50E-06	8.52E-06
1	9.5	0.2	1.48E-06	1.49E-06
2	1.0	1.0	2.43E-05	2.44E-05
2	4.0	0.8	1.33E-05	1.34E-05
3	3.5	0.8	2.11E-05	2.12E-05
3	8.5	0.4	8.28E-06	8.29E-06
4	10.0	0.4	9.86E-06	9.88E-06
4	4.5	0.6	2.09E-05	2.11E-05
5	2.75	0.6	3.22E-05	3.24E-05
5	10.0	0.8	2.01E-05	2.03E-05

autonomous parameters that have the most influence on the seepage results are selected as the input terminals. They include sheet pile's height, upstream water level, and hydraulic conductivity anisotropy ratio of deposit materials. The output terminal is considered a normalized flow rate $Q_{Nor.}$. Table 2 states the range of parameters for the input and output terminals in this research.

For the sake of brevity, a summary of the process is expressed here. One thousand separate analyses are conducted using SBFEM to cover all patterns for different values of the mentioned parameters. To this end, a computer program based on SBFEM was coded

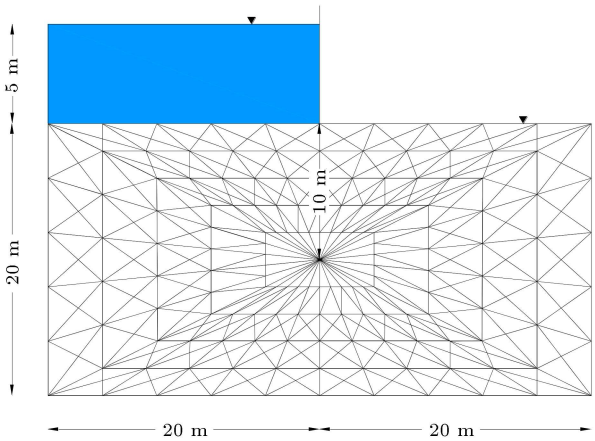

Figure 3. Domain discretization of Scaled Boundary Finite Element Method (SBFEM).

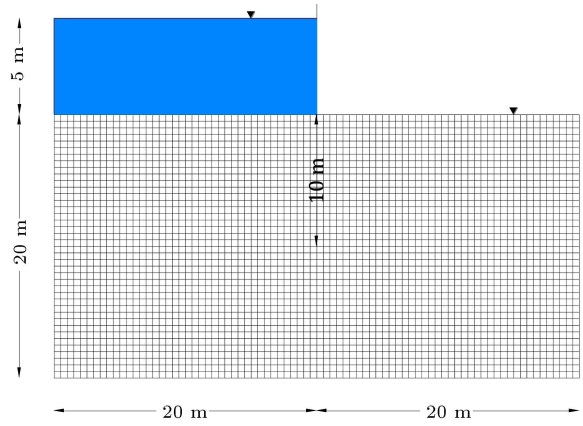

Figure 4. Domain discretization of Finite Element Method (FEM).

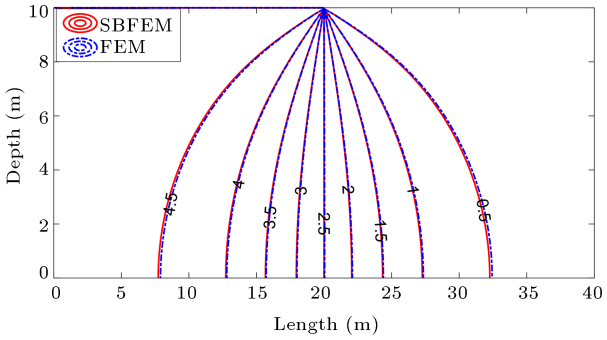

Figure 5. Contour of potential lines.

Table 2. Adopted range of parameters for developing Gene Expression Programming (GEP) model.

Parameters	Range
Input parameters	
Sheet pile's height (D)	0.25–10 m
Upstream level (H)	1–5 m
Hydraulic conductivity anisotropy ratio (k_y/k_x) (K)	0.2–1
Output parameter	
Normalized flow rate $Q_{Nor.}$	1.42E-6–8.54E-5

in MATLAB by the authors. In each scenario, the boundary of the domain is discretized into 450 subdomains. Applying specific boundary conditions in every single scenario and following the SBFEM procedure produced a solution to the seepage problem beneath the sheet pile. Finally, by using the proposed SBFEM model, the normalized flow rate was computed. In order to insert each component of the database at the interval of [0,1], each component is normalized by the max-min technique.

6. Performance analysis

In GEP, values for the model parameters such as numbers of chromosomes and genes and the gene's head size have a significant influence on the fitness of the output model. To find an optimum value for each of the model parameters, one thousand generations were carried out and the values of one of the model parameters varied, whereas the values of the other parameters were kept constant. For each generation, Mean Squared Errors (MSE) in both training and testing sets were recorded so that the values that would give the least MSE could be identified. Typical results of performance analysis for developing a normalized flow rate model are shown in Figures 6, 7, and 8. Figure 6 shows that the model had the best performance when the number of chromosomes was 30. This value corresponds to the least MSE in the training sets. Figure 7 presents the effect of some genes. It can be seen that the GEP model performs best when the gene number is 3. Figure 8 demonstrates the influence of gene's head size on the performance of the model. The optimum relationship for the normalized flow rate was developed based on GEP parameters, as given in Table 3.

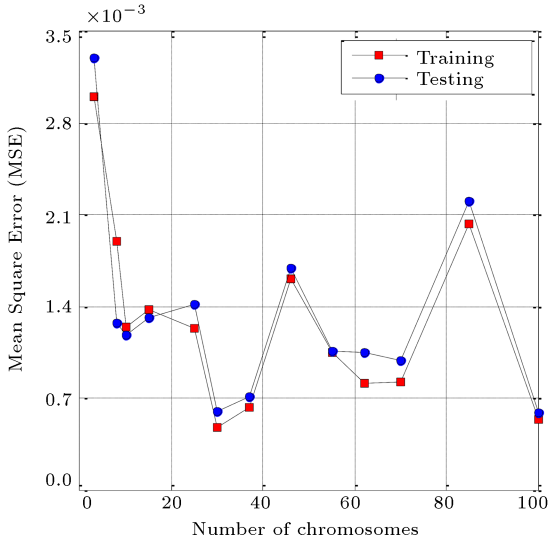

Figure 6. Effect of the number of chromosomes on the performance of the Gene Expression Programming (GEP) model.

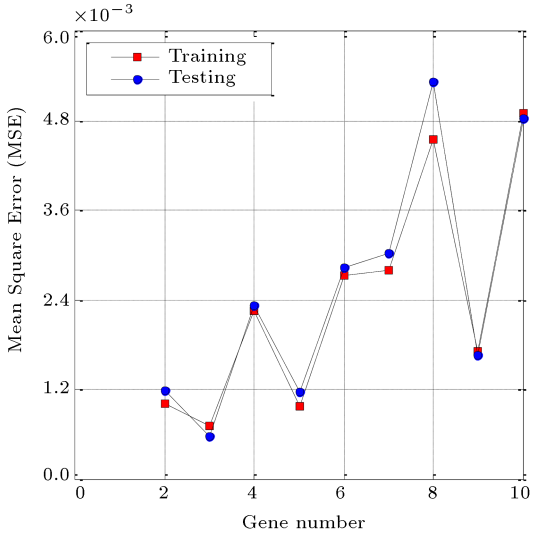

Figure 7. Effect of gene number on the performance of the Gene Expression Programming (GEP) model.

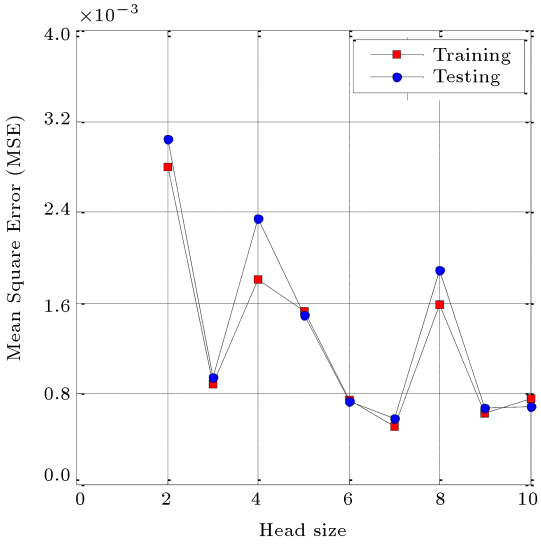

Figure 8. Effect of head size on the performance of the Gene Expression Programming (GEP) model.

7. Model development by GEP

In this research, GEP software, i.e., GeneXproTools 5.0 [38], was used for conducting symbolic regression to find a relationship for a normalized flow rate. As a rule, 80–85% of the database was employed to train the GEM model, while the remaining dataset served to test the proposed model. In this way, a total of 800 results of the SBFEM analysis were employed to train the model (80%). Furthermore, the 200 remaining data were utilized to test the model.

An optimum relationship was achieved by making alterations to the programs such that minimum error could be obtained compared with the actual database. In this process, efficiency was controlled using the sum of absolute differences between the estimated and

Table 3. The utilized Gene Expression Programming (GEP) parameters for the normalized flow rate models.

Parameter	Setting
General	
Function set	$+$, $-$, $\times$, $/$, $\sqrt{}$, X^2, X^3, $\sqrt[3]{}$, $\sqrt[5]{}$, Inv, Not
Number of chromosomes	30
Head size	7
Number of genes	3
Linking function	Addition
Enable complexity increase	Disable
Fitness function	
Fitness function type	Root Mean Square Error (RMSE)
With parsimony pressure	Disable
Genetic operators	
Mutation rate	0.00138
Inversion rate	0.00546
IS transposition rate	0.00546
RIS transposition rate	0.00546
One-point recombination rate	0.00277
Two-point recombination rate	0.00277
Gene recombination rate	0.00277
Gene transposition rate	0.00277
Numerical constant	
Constant per gene	10
Data type	Floating-point
Lower bound	–10
Upper bound	10

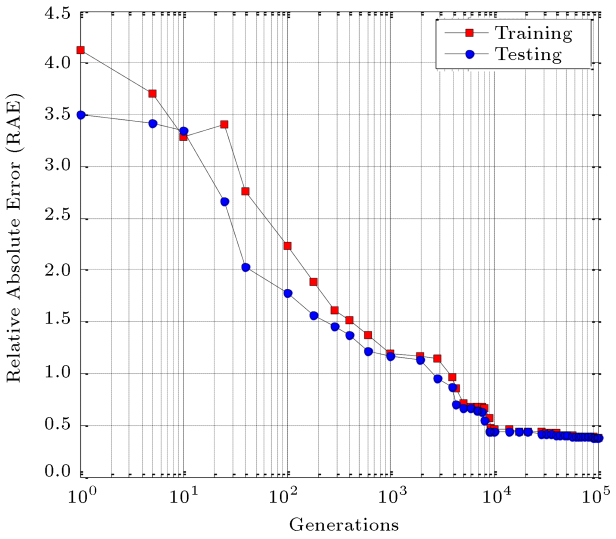

Figure 9. Variation of error measured during training and testing generations..

actual values of the normalized flow rate. Iterations stopped when the error value did not decrease extremely for training and testing data. Figure 9 shows the variations of the relative absolute error in training and testing data while developing the best model for the normalized flow rate. For training data, the error of the model decreased from 4.12 in the first generation to about 0.38 after 100,000 generations. To test the data, the error decreased from 3.49 to about 0.38 for the same number of generations.

GEP constructs Expression Trees (ETs) as the relation between the inputs and outputs of the model. As shown in Figure 10, the appropriate ET of the final modeling contains three subtrees, namely ET1, ET2, and ET3, which are linked to each other by "addition".

The illustrated ETs in Figure 10 are formulated into Eq. (14) used for predicting all 800 and 200 normalized flow rates of the training and testing sets, respectively. In addition, Eqs. (15) and (16) are developed as given in Table 4. However, this equation is selected as the proposed model in this study due to the simplicity of Eq. (14) and the corresponding value of R^2 which was higher than that of others.

Figures 11 and 12 compare the predicted and actual normalized flow rates for training and testing data. There is a good correlation in these figures between the predictions via GEP modeling and the actual data for both training and testing sets.

In these figures, the square correlation coefficient, R^2, is used to compare the results given by:

$$R^2 = 1 - \frac{\sum_{i=1}^{n} (A_i - P_i)^2}{\sum_{i=1}^{n} (A_i - \bar{A}_i)^2}, \tag{13}$$

where A_i and P_i are the actual and predicted output values for the ith output, respectively, $\bar{A}_i$ is the average of the actual outputs, and n is the number of data points.

8. Sensitivity analysis

A sensitivity analysis was performed to assess the model response to the variation of input parameters. To figure out the influence of each input parameter on the normalized flow rate, the mean value of the input parameter increased by approximately 20%, while the values of the other input parameters were kept constant. According to Table 5, the normalized flow rate decreased with an increase in the height of the sheet pile. Furthermore, this table reveals that with an increase in the upstream head and hydraulic conductivity anisotropy ratio, the normalized flow rate increased. As observed, the upstream head plays a key role in the normalized flow rate parameter.

9. Parametric analysis

In this section, a parametric analysis was carried out to verify the proposed GEP model. The main objective of

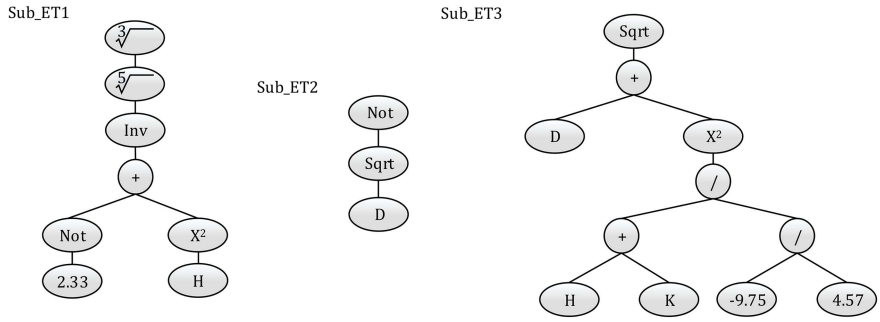

Figure 10. Expression tree of the proposed model.

Table 4. The derived predicted models.

Models	Functions	R^2	Equation nos.
Proposed model $= \sqrt[15]{\frac{1}{K^2-1.33}} + \sqrt{D + \frac{(H+K)^2}{4.53}} - \sqrt{D} + 1$	$+$, $-$, $*$, $/$, Sqrt, X^2, X^3, $\sqrt[3]{}$, $\sqrt[5]{}$, Inv, Not	97.05	(14)
Model 2 $= \left(\frac{0.4H+1.48}{3.71}\right)^{0.25}(D(K-D)) - \frac{(H+D)D}{2.49K} + D^2 + 10^{-(0.69+3.26H)}$	$+$, $-$, $*$, $/$, Sqrt, Exp, Pow10, Inv, X^2	96.71	(15)
Model 3 $= \log\left(\frac{\sqrt[3]{e^K \sqrt[3]{0.34}}}{\log(10)}\right) - \frac{D}{2.17H} + \frac{D}{e\sqrt{H}}$	$+$, $-$, $*$, $/$, Sqrt, Exp, Log, Ln, X^2, X^3, $\sqrt[3]{}$	96.63	(16)

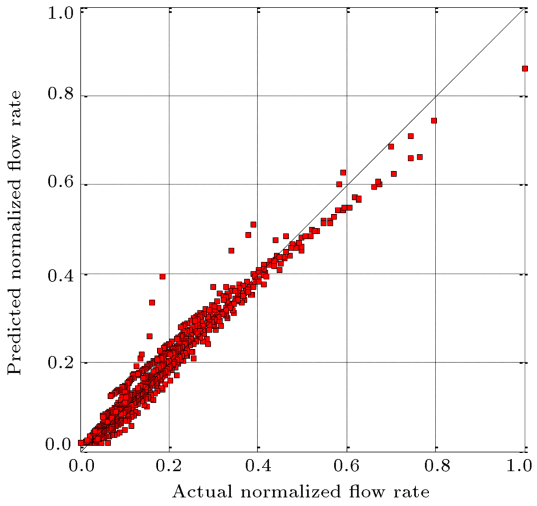

Figure 11. Actual versus predicted normalized flow rate values for training data, $R^2 = 0.966$.

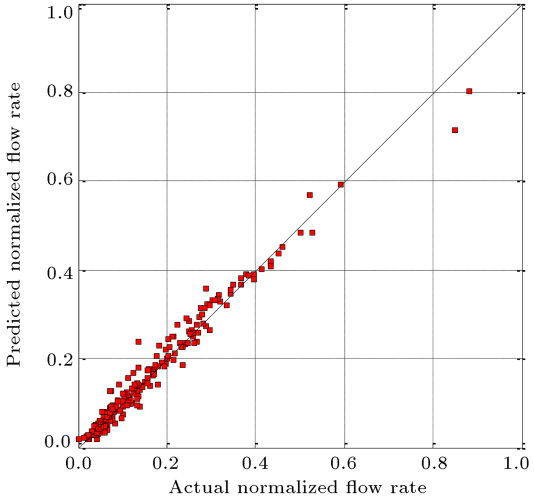

Figure 12. Actual versus predicted normalized flow rate values for testing data, $R^2 = 0.971$.

this study was to evaluate the effects of each parameter on the normalized flow rate beneath the sheet pile. Figures 13–15 show the predicted values for the normalized flow rate as a function of each parameter, while the others are kept constant. According to the results from parametric analysis, as expected, the normalized flow rate beneath the sheet pile increased by increasing the upstream head and hydraulic conductivity anisotropy ratio. Upon increasing the height of the sheet pile, the normalized flow rate

Table 5. The change in normalized flow rate corresponding to change of input parameters.

Parameters	Upstream head (m)	Sheet pile height (m)	Hydraulic conductivity anisotropy ratio
Normalized flow rate	52.39%	–6.70%	17.88%

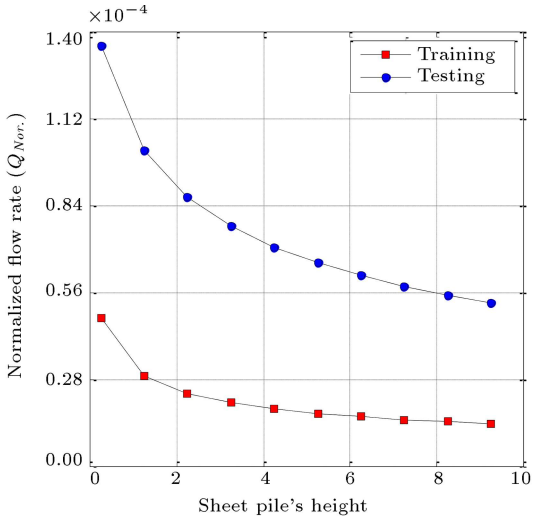

Figure 13. Parametric analysis of output model with respect to sheet pile's height.

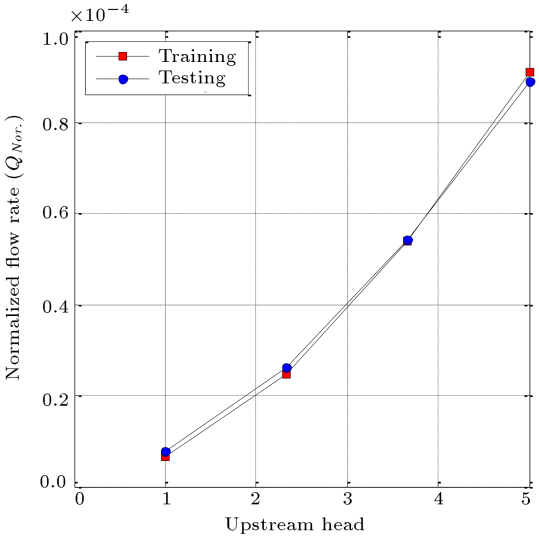

Figure 14. Parametric analysis of output model with respect to the upstream head.

beneath the sheet pile decreased. Based on the slope of the curves, it can be concluded that the upstream head is the most effective parameter with respect to the normalized flow rate beneath the sheet pile.

10. Conclusion

A model based on Gene Expression Programming (GEP) was proposed to predict the normalized flow rate beneath the sheet pile. The input model consisted of upstream head, sheet-pile height, and hydraulic conductivity anisotropy ratio. Since Scaled Boundary Finite Element Method (SBFEM) enjoyed a significant advantage in directly modeling the singular points with high accuracy, this method was utilized to model seepage beneath the sheet piles as a singular point. A database containing the results of 1000 SBFEM models

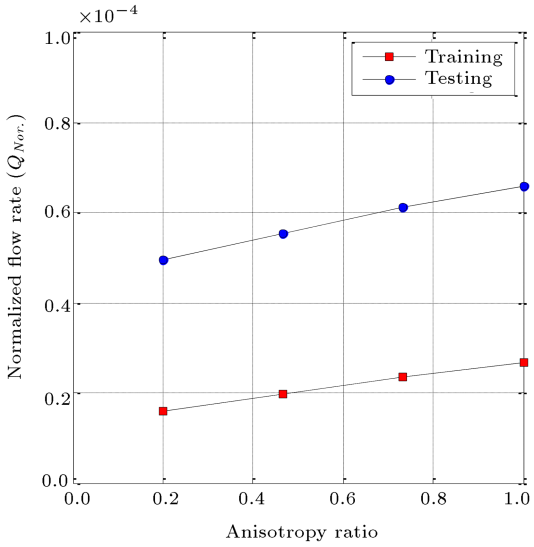

Figure 15. Parametric analysis of output model with respect to hydraulic conductivity anisotropy ratio.

was employed to develop the model. The results from the 800 SBFEM seepage model beneath the sheet pile were used for training the model to determine the normalized flow rate for different input parameters. Further, the model was tested using another database containing the normalized flow rate of 200 obtained from the SBFEM model. To find the optimum values for model parameters, performance analysis was performed. One thousand generations were carried out to find the model parameters. The optimum relationship was obtained by making alterations to achieve minimum error; in this process, the error value did not significantly decrease in the training and testing data sets after 100000 generations.

The model prediction showed reasonable accuracy for both training and testing data. A comparison between the model prediction and actual data showed a good performance in predicting the normalized flow rate. The sensitivity analysis indicated that the upstream head was the most influential parameter in the normalized flow rate. Furthermore, a parametric analysis showed an acceptable trend for the normalized flow rate with changing the input parameters of the model. The authors suggest conducting the following future researches for extension of the topic:

- Developing a prediction model for normalized flow rate in free-surface flow problems with toe drain;
- Extending the prediction model for seepage problems under the concrete dam;
- Assessing reliability of the developed model.

References

1. He, J.H. "Approximate analytical solution for seepage flow with fractional derivatives in porous media",

Computer Methods in Applied Mechanics and Engineering, **167**, pp. 57–68 (1998).

2. Jie, Y., Jie, G., Mao, Z., and Li, G. "Seepage analysis based on boundary-fitted coordinate transformation method", *Computers and Geotechnics*, **31**, pp. 279–283 (2004).
3. Fukuchi, T. "Numerical analyses of steady-state seepage problems using the interpolation finite difference method", *Soils and Foundations*, **56**, pp. 608–626 (2016).
4. Bresciani, E., Davy, P., and Dreuzy, J.R. "A finite volume approach with local adaptation scheme for the simulation of free surface flow in porous media", *International Journal for Numerical and Analytical Methods in Geomechanics*, **36**, pp. 1574–1591 (2012).
5. Ouria, A., Toufigh, M.M., and Nakhai, A. "An investigation on the effect of the coupled and uncoupled formulation on transient seepage by the finite element method", *American Journal of Applied Sciences*, **12**, pp. 950–956 (2007).
6. Kazemzadeh-Parsi, M.J. and Daneshmand, F. "Three dimensional smoothed fixed grid finite element method for the solution of unconfined seepage problems", *Finite Elements in Analysis and Design*, **64**, pp. 24–35 (2013).
7. Rafiezadeh, K. and Ataie-Ashtiani, B. "Transient free-surface seepage in three-dimensional general anisotropic media by BEM", *Engineering Analysis with Boundary Elements*, **46**, pp. 51–66 (2014).
8. Jie, Y.X., Liu, L.Z., Xu, W.J., and Li, G.X. "Application of NEM in seepage analysis with a free surface", *Mathematics and Computers in Simulation*, **89**, pp. 23–37 (2013).
9. Zhang, W., Dai, B., Liu, Z., and Zhou, C. "Unconfined seepage analysis using moving Kriging mesh-free method with Monte Carlo integration", *Transport in Porous Media*, **116**, pp. 163–180 (2017).
10. Song, C. and Wolf, J.P. "The scaled boundary finite-element method-alias consistent infinitesimal finite-element cell method-for elastodynamics", *Computer Methods in Applied Mechanics and Engineering*, **147**, pp. 329–355 (1997).
11. Bazyar, M.H. and Graili, A. "A practical and efficient numerical scheme for the analysis of steady-state unconfined seepage flows", *International Journal for Numerical and Analytical Methods in Geomechanics*, **36**, pp. 1793–1812 (2012).
12. Bazyar, M.H. and Talebi, A. "Transient seepage analysis in zoned anisotropic soils based on the scaled boundary finite-element method", *International Journal for Numerical and Analytical Methods in Geomechanics*, **39**, pp. 1–22 (2015).
13. Johari, A. and Heydari, A. "Reliability analysis of seepage using an applicable procedure based on stochastic scaled boundary finite element method", *Engineering Analysis with Boundary Elements*, **94**, pp. 44–59 (2018).
14. Su, H., Li, J., Wen, Z., Guo, Z., and Zhou, R. "Integrated certainty and uncertainty evaluation approach for seepage control effectiveness of a gravity dam", *Applied Mathematical Modelling*, **65**, pp. 1–22 (2019).
15. Xie, J.X., Cheng, C.T., Chau, K.W., and Pei, Y.Z. "A hybrid adaptive time-delay neural network model for multi-step-ahead prediction of sunspot activity", *Int. J. Env. Poll.*, **28**, pp. 364–381 (2006).
16. Taormina, R., Chau, K.W., and Sethi, R. "Artificial neural network simulation of hourly groundwater levels in a coastal aquifer system of the Venice lagoon", *Eng. Appl. Artif. Intell.*, **25**, pp. 1670–1676 (2012).
17. Azamathullah, H.M.D., Chang, C.K., Ghani, A.A., Ariffin, J., Zakaria, N.A., and Abu Hasan, Z. "An ANFIS-based approach for predicting the bed load for moderately-sized rivers", *J. Hydro-Environ. Res.*, **3**, pp. 35–44 (2009).
18. Azamathulla, H.M.D. and Ghani, A.A. "An ANFIS-based approach for predicting the scour depth at culvert outlet", *J. Pipeline Syst. Eng. Pract.*, **2**, pp. 35–40 (2011).
19. Gao, W. "Premium-penalty ant colony optimization and its application in slope stability analysis", *Applied Soft Computing*, **43**, pp. 480–488 (2016).
20. Ahangar-Asr, A., Javadi, A.A., Johari, A., and Chen, Y. "Lateral load bearing capacity modelling of piles in cohesive soils in undrained conditions: An intelligent evolutionary approach", *Applied Soft Computing*, **24**, pp. 822–828 (2014).
21. Cheng, C.T., Wang, W.C., Xu, D.M., and Chau, K.W. "Optimizing hydropower reservoir operation using hybrid genetic algorithm and chaos", *Water Resources Management*, **22**, pp. 895–909 (2008).
22. Johari, A., Javadi, A.A., and Habibagahi, G. "Modelling the mechanical behaviour of unsaturated soils using a genetic algorithm-based neural network", *Computers and Geotechnics*, **38**, pp. 2–13 (2011).
23. Yalcin, Y., Orhon, M., and Pekcan, O. "An automated approach for the design of mechanically stabilized earth walls incorporating metaheuristic optimization algorithms", *Applied Soft Computing*, **74**, pp. 547–566 (2019).
24. Vardhan, H., Garg, A., Li, J., and Garg, A. "Measurement of stress dependent permeability of unsaturated clay", *Measurement*, **91**, pp. 371–376 (2016).
25. Zhou, W.H., Garg, A., and Garg, A. "Study of the volumetric water content based on density, suction and initial water content", *Measurement*, **94**, pp. 531–537 (2016).
26. Mishra, A.K., Kumar, B., and Vadlamudi, S. "Prediction of hydraulic conductivity for soil-bentonite mixture", *Int. J. Environ. Sci. Technol.*, **14**, pp. 1625–1634 (2017).
27. Gandomi, A.H., Alavi, A.H., Mohammadzadeh-Shadmehri, D., and Sahab, M.G. "An empirical model for shear capacity of RC deep beams using genetic simulated annealing", *Arch Civil Mech. Eng.*, **13**, pp. 354–369 (2013).

28. Johari, A., Habibagahi, G., and Ghahramani, A. "Prediction of SWCC using artificial intelligent systems: A comparative study", *Scientia Iranica*, **18**, pp. 1002–1008 (2011).
29. Johari, A., Habibagahi, G., and Ghahramani, A. "Prediction of a soil-water characteristic curve using a genetic-based neural network", *Scientia Iranica*, **13**, pp. 284–294 (2006).
30. Azamathulla, H.M.D., "Gene-expression programming to predict friction factor of Southern Italian Rivers", *Neural Comput. Appl.*, **23**, pp. 1421–1426 (2013).
31. Guven, A. and Azamathulla, H.M.D. "Gene-expression programming for flip bucket spillway scour", *Water Sci. Technol.*, **65**, pp. 1982–1987 (2012).
32. Azamathulla, H.M.D. "Gene expression programming for prediction of scour depth downstream of sills", *J. Hydrol.*, **460**, pp. 156–159 (2012).
33. Marino, M.A. and Luthin, J.N., *Seepage and Groundwater*, Elsevier (1982).
34. Wolf, J.P., *The Scaled Boundary Finite Element Method*, John Wiley & Sons (2003).
35. Wolf, J.P. and Song, C. "The scaled boundary finite-element method-a fundamental solution-less boundary-element method", *Computer Methods in Applied Mechanics and Engineering*, **190**, pp. 5551–5568 (2001).
36. Song, C. and Wolf, J.P. "The scaled boundary finite-element method: analytical solution in frequency domain", *Computer Methods in Applied Mechanics and Engineering*, **164**, pp. 249–264 (1998).
37. Ferreira, C. "Gene expression programming: A new adaptive algorithm for solving problems", *Complex Syst.*, **13**, pp. 87–129 (2001).
38. GEPSOFT. GeneXproTools. Version 4.0, http://www.gepsoft.com.

Biographies

Ali Johari obtained his BS, MS, and PhD degrees in 1995, 1999, and 2006, respectively, from Shiraz University, Iran, where he is currently an Assistant Professor at the Civil and Environmental Engineering Department. He was a Post-Doctoral Researcher at Exeter University in 2008, where he is also a member of the research state of the Computational Geomechanics Group. His research interests include unsaturated soil mechanics, application of intelligent systems in geotechnical engineering, probabilistic models, and reliability assessment. He has also consulted and supervised numerous geotechnical projects.

Ahmad Heydari graduated from Shiraz University of Technology, Shiraz, Iran in 2018. He has authored several papers on numerical method and uncertainty analysis. Right now, he is the C.E.O of the Joosh Payesh Khorasan Company, Mashhad, Iran (soil, concrete, and weld laboratory) and a advisor to several companies. The main interests are numerical modeling and artificial intelligence.

Abbas Talebi was born in 1987 in Shiraz, Iran. He graduated from Hormozgan University in Civil Engineering with BS degree in 2010. He obtained his MS degree in Geotechnical Engineering from Yasouj University in 2013. Currently, he is furthering his geotechnical engineering education at Shiraz University of Technology as a PhD candidate. His main research interests include numerical methods in geotechnical engineering, slope stability analysis, piled raft foundations, unsaturated soils, and reliability analysis.